Diyala Journal of Engineering Sciences

Journal homepage: https://djes.info/index.php/djes

ISSN: 1999-8716 (Print); 2616-6909 (Online)

Transient Simulation of a Permanent Magnet Synchronous Motor Utilizing *V/f* Control Aligned with the Park Transform

Mohammed S Hasan*, Assama S. Jafar, Ahmed I Jabber

Department of Power and Electrical Machines, College of Engineering, University of Diyala, Iraq

ARTICLE INFO

Article history:
Received September 18, 2024
Revised June 23, 2025
Accepted July 19, 2025
Available online September 01, 2025

Keywords:
Permanent magnet synchronous motor (PMSM), Park's transforms, ,Stationary frame αβ ,Exited frame *dq* ,Transients period, *V/f* controller Dynamic Model, MATLAB/Simulink

ABSTRACT

Permanent magnet synchronous motors are widely used in industrial laboratories due to their high starting torque and efficiency compared to static induction machines. The growing interest can be explained by the development of permanent magnet magnetic materials. To evaluate the transient behavior of permanent magnet synchronous motors, a MATLAB model is considered based on the Parke transform to simplify the control strategy that implements voltage-to-frequency (V/f) ratio to maintain more stability during unsteady conditions and facilitate the analysis to track the machine action. Managing this transient phase is essential to prevent excessive inrush currents and ensure stability. This study rigorously examines the behavior of machines during two transition periods until they reach a steady state speed. The rise time (Tr) is the time it takes for a signal to change from (10 - 90) % of its final value. The transient speed duration of the first approach varies between 0.4 ms for the unloaded machine and performs longer duration time 0.7 ms under load conditions. The unloaded machine obviously responds faster than the loaded machine .The second, controlled approach has a limited duration time periods from 10.25 to 10.8 ms, with a rise time of Tr1 = 0.2ms and Tr2 = 2,5ms for both loads applied sequentially. The controlled machine demonstrates a shorter rise time which can be attributed to the same speed root forced to different load conditions. This approach highlighted the benefits of the inherent dc boost voltage to minimize transient effects in synchronous machine.

1. Introduction

A Permanent Magnet Synchronous Motor (PMSM) is an AC motor uses permanent magnets embedded in the rotor to create a constant magnetic field [1]. The machine is made from high-performance permanent magnets, such as neodymium or ferrite, to maintain synchronization with the stator's rotating magnetic field [2]. Permanent magnet motors are characterize by a simple structure, small size, and lightweight design, making them ideal for wind power conversion systems and electric vehicles. Brushless operation is one of the key features of PMSM. Since they do not have brushes, they require less maintenance and offer higher reliability [3]. The machine in motoring mod PMSM is widely utilized in many applications such as Computer Numerical Control CNC machines, industrial robots, and electric drives [4]. The PMSM offer better

* Corresponding author.
E-mail address: mssh6144@gmail.com
DOI: 10.24237/djes.2025.18311

efficiency compared to induction motors due to the elimination of rotor copper losses. The machine is characterized by high magnetic density, so it is preferred to use strong permanent magnets, resulting in a compact design with a high torque-to-weight ratio. Permanent synchronous machine─easy deals with many control theories so the machine is widely used in applications requiring precise speed and position control, such as robotics. [5],[6]. The machine gained widespread attention due to certain features such as high torque/ inertia ratio, high power to obtain the highest performance value [7]. Working Principle: The stator of a PMSM is like that of an induction motor, with three-phase windings that generate a rotating magnetic field when AC power is supplied. The rotor, equipped with permanent magnets, follows this field synchronously without slip, meaning the rotor speed is directly proportional to the supply frequency. Due all this PMSM features widely used in many Applications such Electric Vehicles (EVs) and Hybrid Vehicles, Industrial Automation and Robotics, Aerospace and Wind Energy, HVAC Systems and Home Appliances PMSM are favored for their high efficiency, compact size, and precise control, making them ideal for modern energy-efficient applications. Simulation can be used to evaluate variations in electrical parameters under different loading conditions, making PMSM valuable for educational and laboratory research [8]. All these advantages lead to the use of the angular transformation of the voltage axes and current vectors as a multiple coordinate frame. Especially for three-phase machines. It is then possible to run the frame on these DC quantities before back-converting to restore the actual three-phase AC current. This transformation is called the Park transformation [9]. This poses a major challenge to the role of power electronics applications to refine the start-up performance of the machine due to unstable start-up machine periods that are characterized by random disturbances, when the machine trying to reach steady state speed [10]. Accordingly, some incorporate squirrel cages established in the rotors construction for starting period requirements, which are known as line-start or self-starting PMSM [11]. These are typically used as high-efficiency replacements for induction motors to simplify the startup operation periods based on PMSM [12]. The configuration of concerned permanent magnet PMSM machine described in figure 1 below:

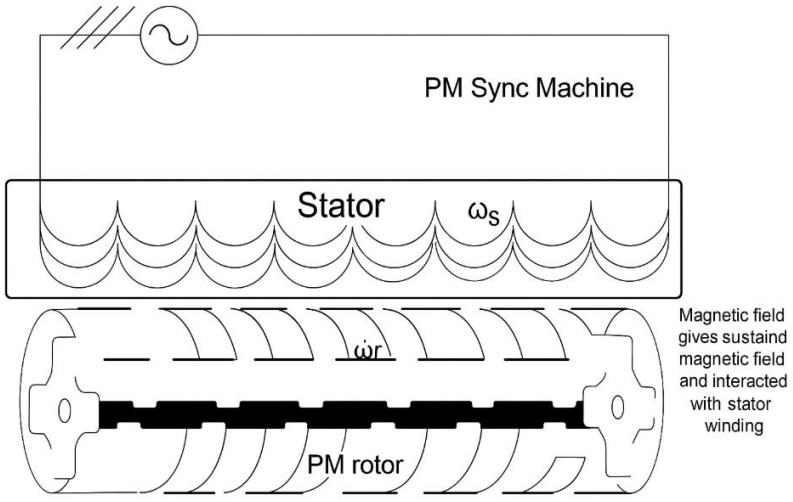

Figure 1: Configuration of PM synchronous Machine.

Where ω_s -Stator angular speed(rad/s), ω_r - rotor angular speed (rad/s). The starting process has a critical phase that the motor rid through, especially for permanent magnets manufacturing as axial flux synchronous motor. This individual process is more complicated than a common induction machine [13]. Obviously, the magnetic field produced by the permanent magnet is a constant magnetic field

and has no symmetry in the magnetic field possessed by the rotor of the induction machine; therefore, the comparative study with common induction machines, suggested the turned rod positions of rotors. So, on the stator; apply the correct three-phase alternating current and starting voltage, to make the paramagnetic synchronous motor starting [14].
Building simulation models for a specific SC control algorithm is an important way to analyze a PMSM model and evaluate the behavior of a machine during power flow between the stator and rotor [15].
Also, the equation of the mathematical dynamic model of the machine needs the benefits of dq frame of Parkes transformation to simplify the math equations in a low-order form, suitable to use as a core requirement in simulation software [16].

The transient behaviors that appeared during the control processes are also part of this study, as they help test control and machine stability. The simulation figures appearing in both approaches will outline each parameter associated with the scalar control algorithm under different load conditions. There are custom tests of the machine during two transient periods: the first approach is without control presented the natural behaviors of the parameter under start up condition when the machine tries hard to match the steady state condition under a half-loaded machine under *scalar* control [16].
The advantages of the Parks transform became crucial for low-order (*d-q*) control operations, prompting the researchers to clarify the key steps to match the steady state condition with basic control algorithms such V/f controller. This approach provides more accurate details during the transient period in active and reactive power in the simulation model.

This research aims to significantly enhance the performance of permanent magnet machines through a groundbreaking control simulation method designed to optimize their operation during critical transient periods. The study rigorously analyzes the dynamics of PMSM during two key transitional phases. The first phase, marked by inherent instability at startup machine, shows that speed rise times are influenced by load conditions and motor design, underscoring the need for tailored solutions for optimal performance. Studying transient states in electrical machines is an advanced step toward obtaining accurate electrical properties. The use of this control algorithm aims to simplify this process by relying on reliable sources. This study emphasizes the need for energy researchers to cultivate an analytical culture that combines advanced control methods with simulation. Engaging with research on electrical power machines can lead to significant advancements in the power field.

The first section offers a comprehensive literature review of existing studies that validate this approach, illustrating the machine's robust capacity to effectively tackle related challenges. The second section of the paper structure utilize the principle of estimating of 3PH voltage from the control out comes. The third section contains Park's theory, the frames it has, and the method of transitioning frames from stationary to rotating frame position. Forth section following and defining changes based rotating frame. Forth section is exploiting dynamic model and illustration of the mathematical model of a permanent magnet machine together with control algorithms. Fifth section is counting the simulation result for both transient approaches and finally the conclusion.

2. PMSM under Low Order *d-q* Frames.

Most three-phase machines have a 120° phase gap to represent the triplet of a standard 3PH voltage. Each phase typically requires its equation models, making mathematical formulation one of the most challenging aspects of electromagnetic machine calculations, particularly for tuning and designing control algorithms. [17]. the three-phase mathematical equations are reduced to a two perpendicular-frame axis presented in the simulation model. Thus, attempts to describe the power flow take a more time to solve mathematically. According to the mathematical theory suggested by Park's hypothesis, the phase difference shifts by μ (120) º [18]. The mathematical equations are

derived based on the controller outputs virtual to ratio voltage (V_r) and radian frequency (ω), to estimate the 3ph voltages (1).

$$V_r = \frac{2}{3}\left(V_a e^{j0} + V_b e^{j\frac{2}{3}\pi} + V_c e^{(j\frac{2\pi}{3})^2} \right) \quad (1)$$

where V_a,V_b,V_c three phase voltages (volt). Here, the phase gap μ sequence between the three-phase voltages by (0,120º, 240º). This ensures a stable source supply system, giving Vr more uniform impacts by minimalizing the inherited instabilities appears in scalar control performance as shown in Equation (2).

$$\begin{cases} V_a = V_a(j0) = V_a \\ V_b = V_b(j120) = \mu V_b = V_b \\ V_c = V_c(j240) = \mu^2 V_c = -V_c \end{cases} \quad (2)$$

The proposed control adopted in this study is scalar control [19]. So the expected parameters as the outcomes of control operation is voltage and frequency manipulated with μ as Phase gap between estimated three phase voltage components described in (2). This transformation from complex control voltage *v/f* to 3PH voltage has extremely impact as a flexible way to recover simulation requirements figure 2.

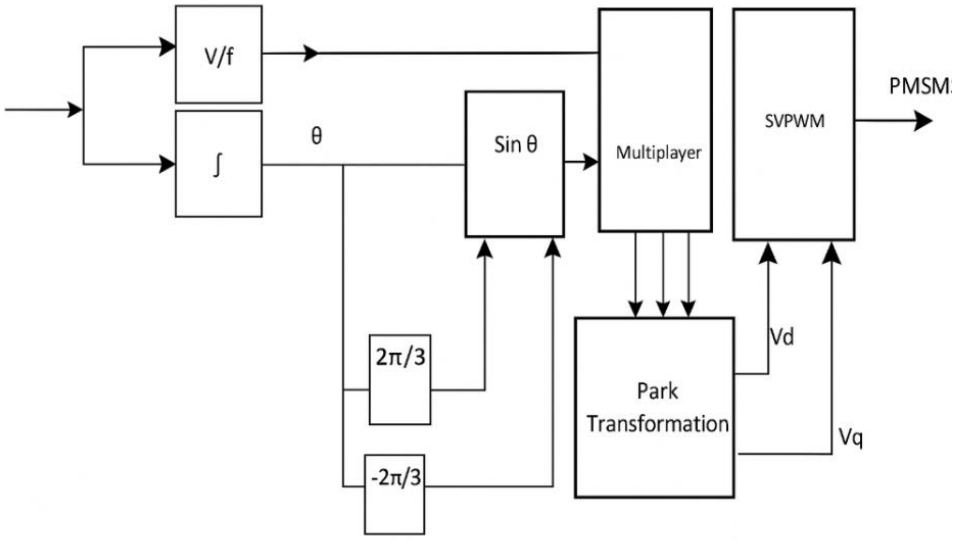

Figure 2: Simulation units of estimating 3phase voltages

The figure 2 Simulink is used to estimate three-phase voltage as a preliminary step based on Park's transformation. Takes in account the advantages of the μ phase gab to build sequential phases with further permanency sidestepping the complex form of scalar control component outcomes, such (voltage, frequency) represented by constant ratio *V/f* [20]. The basic concept of converting the outcomes of the scalar control represented by complex rated voltages V_r and radian frequency ω prepared to provide the second requirements for the conversion developed by the phase angle value to variable three-phase voltages. After sorting the components of the mathematical equation (2)according to their real and imaginary values, the *dq* voltage equation becomes as follows

$$\begin{cases} V_d = \frac{2}{3}V_a - \frac{1}{3}V_b - \frac{1}{3}V_c \\ V_q = \frac{1}{\sqrt{3}}(V_b - V_c) \end{cases} \quad (3)$$

Where V_d, V_q—rotating coordinate voltages, the magnitude of the *dq* voltages can determine by (4)

$$|v_r| = \sqrt{v_q^2 + v_d^2} \quad (4)$$

Then the frame angle can be extracted as:

$$\theta = \tan^{-1}\left(\frac{v_q}{v_d}\right) = \omega t = 2\pi ft \quad (5)$$

The phase angle θ can be presented in stationary θ_s or shafted to the rotating frame with prime mover rotation as exiting θe frame is viewed in figure 3.

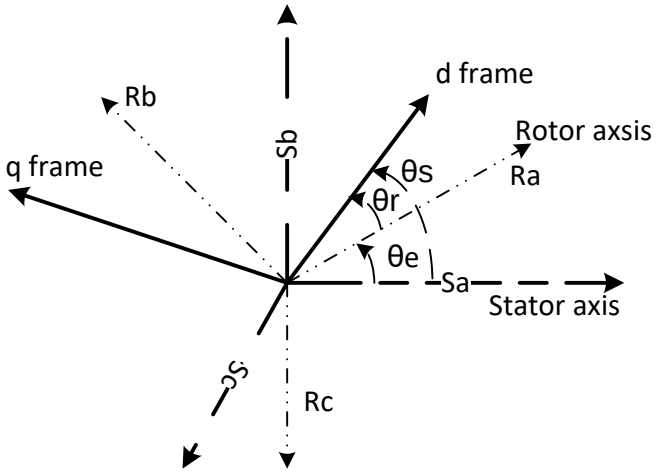

Figure 3: Frame angle displacement θ

3. The Rotating Frame Pacts

In a Permanent Magnet Synchronous Motor (PMSM), the frame angle, represented as **θ** or **϶**, unequivocally determines the orientation of the d-axis and q-axis in relation to the stator's a-phase winding. This angle is vital for maximizing the motor's torque and speed, as it facilitates precise adjustments of the stator voltage components (vd and vq) within the d-q reference frame. By mastering the control of the frame angle, one significantly enhances the motor's performance and efficiency, making it a fundamental aspect of effective motor operation. A change in the machine's acceleration imposes a more modification in the level of vector properties of the electromagnetic parameters voltages, currents and fields. That led to a change in the quadrature coordinates and the frame angle from stationary state θ_s in 2-axis relative to the rotating frame θ_e [21]. Therefore, by succeeding the d-q frame becomes clear that there is a novel role of the angle θ to build successful control. The transient variations in the rotating (*d, q*) frames are directly related to the machine's variable-speed performance [22].

The main objective of scalar control is to maintain a constant magnetic field strength in the motor, resulting in steady torque production. The simulation model figure 4, shows the adapting the rated voltage value (V_r) and the radian frequency ω as essential start step to establish 3 phase voltage and then two axis voltage named by *d-q* coordinates that are required as step dawn order of the control equations and appropriate with the PMSM drive as dynamic model equations [23].

Applying a DC boost voltage to the PMSM enhances its ability to track the source frequency, improving its synchronous characteristics. That's an advantage to achieve a steady state speed, simply without being machine affected by the load change condition. The relative voltages seen in the equation (6) correlating with *V/f* constant, to enhance the stability of the control system as it acquires synchronous properties [24].

$$V_r = \frac{V}{f}\omega_r \tag{6}$$

$$\theta = \int \omega_r dt \tag{7}$$

where, the angular velocity ωr and rotating angle θ are considering the mine production of scaler control unit Figure 4.

The benefit of this equation comes from its impacts on the value of boosting DC voltage required in scalar control. The pivotal value of rotating frequency ωr comes from an ability of a control algorithm to adjust the suitable DC voltage. That motivates the scalar control to maintain the synchronous mode, when the $\omega_r=\omega_s$. Obviously then the machine reached steady state speed and did not need additional DC voltage [25]. On the other circumstance when the rated angular frequency ωr has any

deviants from synchronous frequency $\omega_r \neq \omega_s$ the machine then has an ability to drive speed up or down synchronous depending on the sign of the error in frequency, the DC-DC buck-boost converter adjusts the voltage, controlled via the SVPWM method–to step up or down voltages accomplished with control voltage Figure 4.

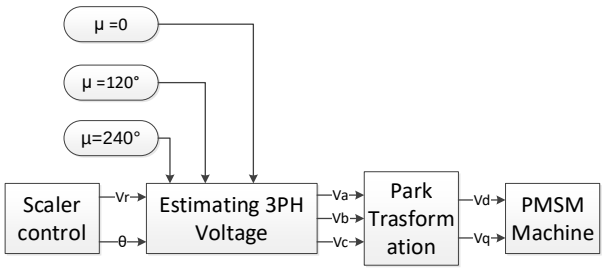

Figure 4: Scenario of presenting Rated voltage in dq frame to drive the machine.

The first modification begins with the 2-axes (α, β) procedure starting from a stationary frame denoted ***s*** sign when the gab angle (θ_s=θ=0). The perpendicular vectors in the rotation farm presented in (*d*-*q*) frame. Then the rotor side of the PMSM machine expressed as an exciting frame noted *e* when ($\theta \neq 0$), depending on the value of the flexible speed [26]. Then the perpendicular coordinates of the rotating vector's voltage are presented as (*d, q*) form. Hence the change in frame state θ_e providing a flexible frame capability to follow the power flow transitions inside machine [26].

The principle at hand addresses a critical concern regarding the effectiveness of enhancement *v/f* constant ratio control algorithms in high-performance simulation control systems. Researchers are deeply invested in the quality of these algorithms, particularly in their ability to effectively regulate voltage, current, and flux in essential frame components, such as α-β, derived from precise phase voltage and current measurements. This regulation is vital for implementing a robust *d*-*q* model based on Park transforms, ensuring optimal steady-state performance and managing limited transient periods in motor operating conditions that encompass both active and reactive parameters [27].

To tackle these challenges, mathematical equations were meticulously crafted to develop a sophisticated MATLAB/Simulink model of Permanent Magnet Synchronous Motors (PMSM). By employing the low-order dq frame, which can be reliably derived through Park Transformation, we can significantly enhance our understanding and control of these complex systems. This approach not only bolsters the performance of PMSM but also aligns with industry demands for precision and efficiency. So the SVPWM inverter can avoids difficulties of using linear functions in a high dimensional space, also it effectively utilizes DC input voltage and reduces THD values. So, observe the machine under a *d, q* frame even thru variable loading conditions is possible. The equivalent circuit of the PMSM dynamic model shown in Figure 5 below edited without losses to prevent control from sudden collapse.

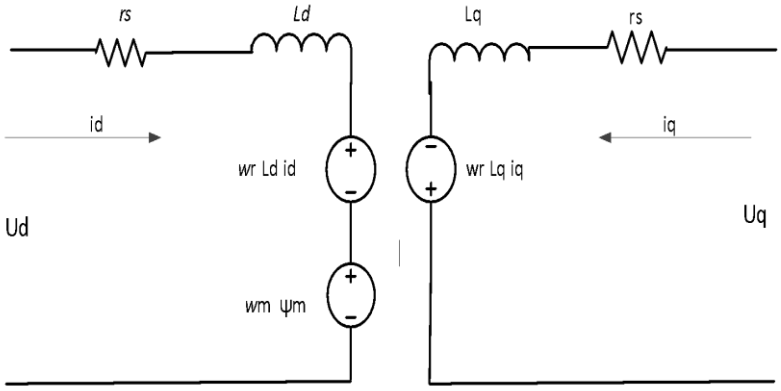

Figure 5: The equivalent circuits for the PMSM without copper losses.

4. Dynamic Model of the PMSM:

The mathematical model for the line-start permanent magnet motor is illustrated in Figure 5. This advanced motor is engineered for self-starting capability when connected to a fixed frequency power supply, ensuring reliable operation. The rotor houses embedded permanent magnets that deliver synchronous excitation, while the rotor cage generates essential induction motor torque for a powerful start. Notably, the significant difference in permeability between the magnet and rotor core enhances magnetic saliency and produces reluctance torque at synchronous speed, showcasing the motor's exceptional performance and efficiency [28]. The conventional construction mode as illustrated in Figure 1 is noted that the main equations to simulate the PMSM are based on flux linkages and currents using low order *d-q* model.

Applying Park's transformation to the block electrical equations produces an expression for torque that is independent of the rotor angle. Park's transformation is defined by [29]:

$$\begin{bmatrix} V_d \\ V_q \\ 0 \end{bmatrix} = \frac{2}{3} \begin{bmatrix} \cos\theta_e & \cos\left(\theta_e - \frac{2\pi}{3}\right) & \cos\left(\theta_e + \frac{2\pi}{3}\right) \\ \sin\theta_e & \sin\left(\theta_e - \frac{2\pi}{3}\right) & \sin\left(\theta_e + \frac{2\pi}{3}\right) \\ 0.5 & 0.5 & 0.5 \end{bmatrix} \begin{bmatrix} V_a \\ V_b \\ V_c \end{bmatrix} \quad (8)$$

where θ_e is the electrical angle using Park's transformation on the stator winding voltages and currents transforms them to the frame, which is independent of the rotor angle:

$$T_e = \frac{2}{3}\omega_r (L_d i_q - L_q i_d) \quad (9)$$

where, T_e— electromagnetic torque (Nm), L_d, L_q ,*d*-axis and *q*-axis inductances, i_q, i_d, *d*-axis and *q*-axis currents. The winding currents, electromagnetic torque and speed equations can be expressed in terms of flux linkage [30].

$$i_q = \frac{\psi_q - \psi_{mq}}{x_{ls}} \quad (10)$$

$$i_d = \frac{\psi_d - \psi_{md}}{x_{ls}} \quad (11)$$

$$T_{em} = \psi_d i_q - \psi_q i_d \quad (12)$$

Where ψ_d , ψ_q - permanent magnet flux linkage for the d, q axis, ψ_{mq} , ψ_{md} -

ω_{rm} : Mechanical velocity of the rotor can be defined correlating with torque.

$$\omega_r = \frac{p}{2}\omega_{rm} \quad (13)$$

The mechanical torque T_e of the PMSM using the torque equation in the *d-q* rotor reference frame:

$$T_e = \frac{3p}{2}\left(\psi_m i_q + (L_d - L_q)\right) i_d i_q \quad (14)$$

where ψ_m — mutual linkage flux, *p*— number of pair pole. To get a clear understanding of the effectiveness of Park's hypothesis to deal with the terms of active and reactive power and show the transient period in its real dimensions as real and imaginary values as they appear in the equations and simulated results. The stator active and reactive power taken by the machine can be represented by the following equations*:*

$$P = V_{ds} i_{ds} + V_{qs} i_{qs} \quad (15)$$

$$Q = V_{qs} i_{ds} - V_{ds} i_{qs} \quad (16)$$

Where's sign "s means orthogonal *d-q* currents and voltages of the stator winding required to build active and reactive power.

5. Simulation Results and discussions.

In this section, a simulation study of a 4 per-pols rotor (8 poles), motoring mod and synchronous speed 750 [rpm] carried out using the initial parameters which is given in Table (1). These sequential simulation results illustrate how the machine recovers from any unsteadiness that appears during the control—process The (MATLAB) software simulations model is simple, stiff and cheap suggested to handle the machine under variable load conditions. As well there is urgent need for adopting (a *V/f* method) to observe a steady state circumstance. According to the results displayed in this paragraph, are possible to obtain the

compensatory values for the machine's performance in the form of *d*, *q* equations as well as the unrest response of the motor under different load conditions.

Table 1: Machines parameters of the PMSM [29]

Symbol	Name	Value
V_{LL}	Rated Voltage	238V
P	Rated Power	1.5 KW
f	Frequency	50 Hz
x_{ls}	Stator Leakage Reactance	1.196 Ω
r_s	Stator resistance	0.3128 Ω
x_d	Stator d-axis reactance.	9.9912 Ω
x_q	Stator q-axis reactance.	19.9824 Ω
r'_{kd}	*d*-axis rotor resistance	0.9936 Ω
r'_{kq}	*q*-axis rotor resistance	1.9872 Ohm
x'_{lkd}	*d*-axis rotor leakage reactance	2.4288 Ohm
x'_{lkq}	*q*-axis rotor leakage reactance	2.4288 Ohm
H	Inertia constant	0.3 s
D_w	0	0

Figure 5 shows the mathematical model of a direct-drive permanent magnet motor. This motor is self-starting when powered by a constant-frequency power supply. Magnets are integrated into the rotor. The permanent magnets provide synchronous excitation, while the rotor cage provides the starting torque of the induction motor.

Figure 6 vividly illustrates the total velocity curve, serving as a clear and compelling indicator of the critical unsteady period during which the machine accelerates to its synchronous velocity. This essential phase, known as "machine start-up," is characterized by significant disturbances in machine behavior and critical vibrations. As a result, experts in this field strategically reserve control techniques for implementation only after the machine has successfully reached a stable state, ensuring optimal performance and safety. When the machine reaches steady-state operation a *scalars* control will be applied to enhance the machine response, by utilizing synchronous mode and its advantages to improve speed response during control processes. Figure 6 as well proves that the machine is exposed to other transient unrest periods, when the machine loses its synchronous characteristics under control condition. The both approaches' will be investigated separately under different load conditions.

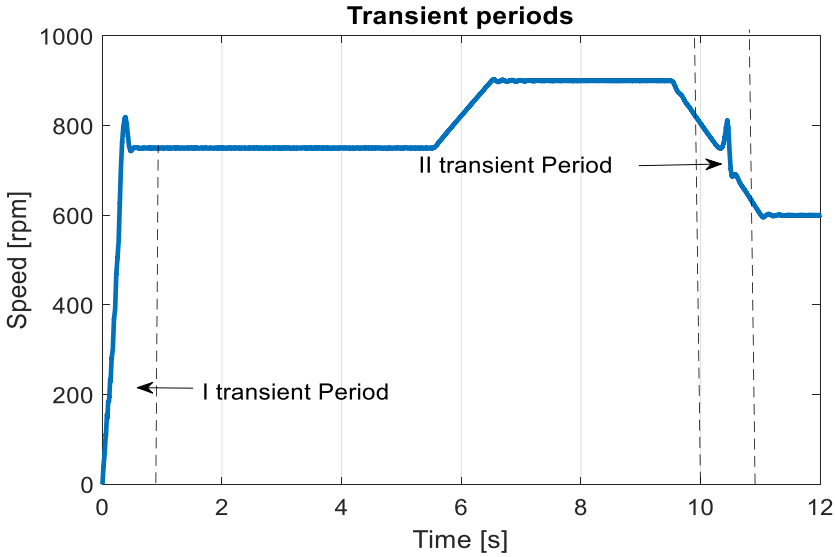

Figure 6: The transient periods appears in PMSM during the simulation model.

First Approach: The machine was tested under unstable and uncontrolled conditions due to the challenges posed by unexpected parameter fluctuations. it was isolated to prevent any damage occurs to the connected drivers. This procedure is common at the beginning of control operations. Additionally, to assess the Permanent Magnet Synchronous Motor's (PMSM) readiness under varying loads. The performance of the PMSM is illustrated by a series of figures obtained from the simulation. The transient response of the machine at startup, under no-load and half-load conditions, was measured at 9 N/m.

The machine primarily monitors stator currents, which reflect the transient behaviors shown in Figure 7.

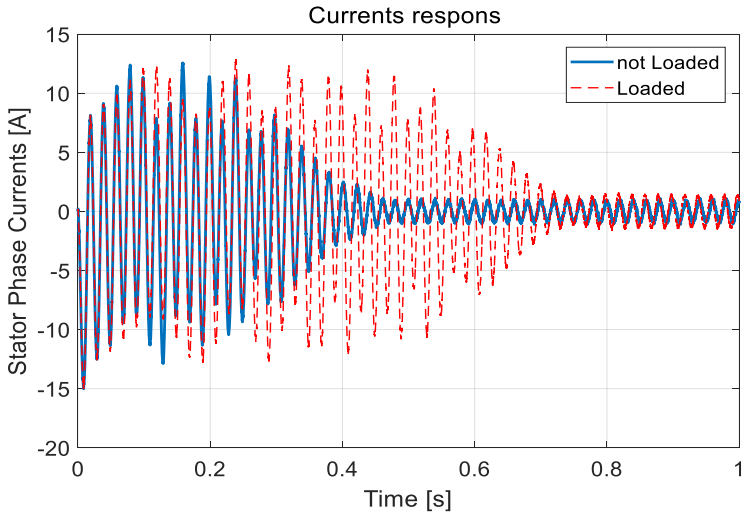

Figure 7: PMSM phase a stator current at variable loaded machine

Figure 7 showed the evaluation study about phase currents are strained by the machine stator at both no-load and half load together when starting from stand still to requested speed the machine takes a different rise time of transient period response 0.44 ms based unloaded machine and 0.77 ms under half loaded machine. . The transient currents indicate that the duration of half-loaded machine is longer than unloaded machine.

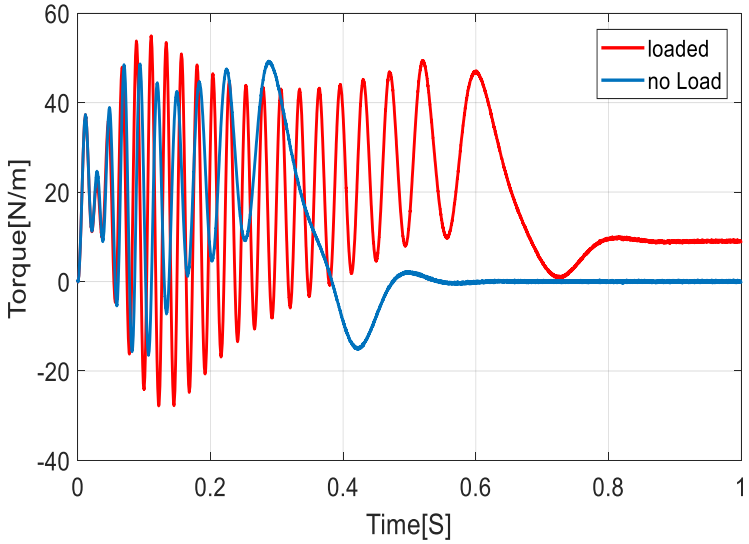

Figure 8: The torque response of PMSM under variable Load condition

The figure 8 shows as well the side of electromagnetic torque (T_{em}) developed by the motor in no-load and half load conditions respectively. It's clearly prove that after the transient period the torque descended to zero case unloaded condition while the load torque

of the machine settles down to meet 9 [N/m], as the record of the value of half-rated load torque. The transient periods of loaded machine appears longer than unloaded machine by 3.6 ms and the unloaded torque settle down to 0 in 0.44 ms but the loaded value match 9N/m after time duration of 0.8ms .

Figure 9 shows the (active) power drawn by the machine in both loading conditions. The figure reflected the deference in consuming reactive power required for machine startup (3000-4000) Wat as not loaded and loaded machine sequentially. The fall time of transient response ended to steady state (0) Wat related to unloaded PMSM machine and 500 Wat with loaded machine the figure as well conform the deference of rise time between the active power trajectory under deferent load conditions.

While in figure 10 has illustrated the reactive power Q under different load conditions. The consuming reactive power is starting from same level at 1500 VAR. The transient clearance time of reactive power case loaded machine is longer than not loaded case.

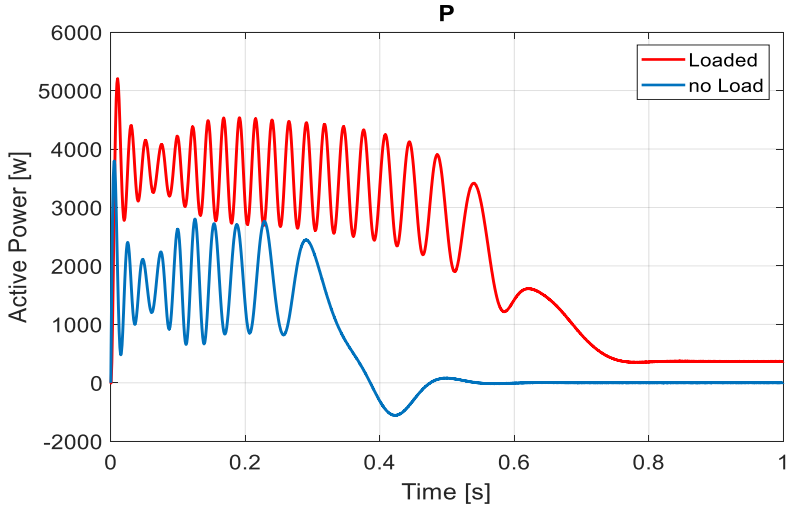

Figure 9: Active power under deferent load condition.

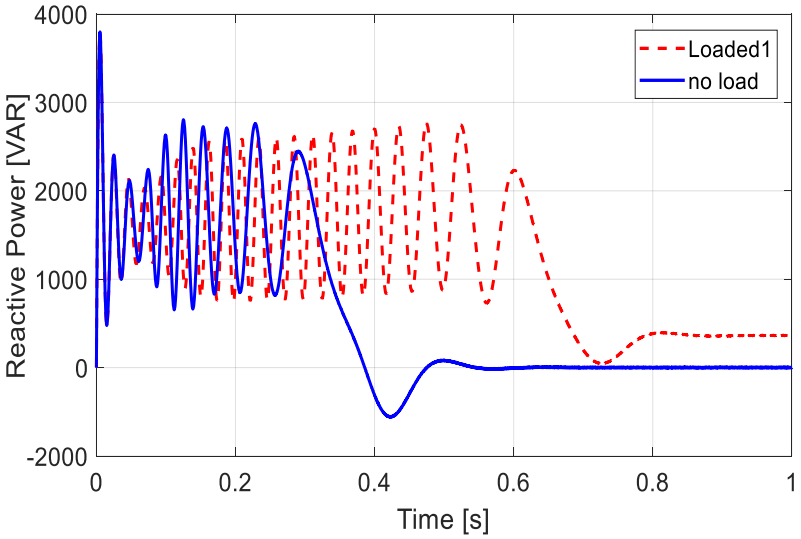

Figure 10: Reactive power under different Load condition

The reactive power in no load and loaded is shown in Figure 10. The behaviors of reactive power in transient period prove obviously that the PMSM are highly efficient machines (low reactive power) and this is one of the main reasons for their importance.

In the last set of simulation results based on uncontrolled conditions. The figure 11 clearly

illustrates the difference in speed paths due to load variation. Describes the speed trajectory of the rotor measured in [rpm] for both load cases. The machine reached the 750 [rpm] with a lagging loaded speed curve in red color. The rise time Tr of not loaded machine is 0.38ms shorter than loaded machine 0.7ms respectively as it clearly measured from figure 11. It confirms a clear difference in the response time between an unloaded machine and its loaded counterpart.

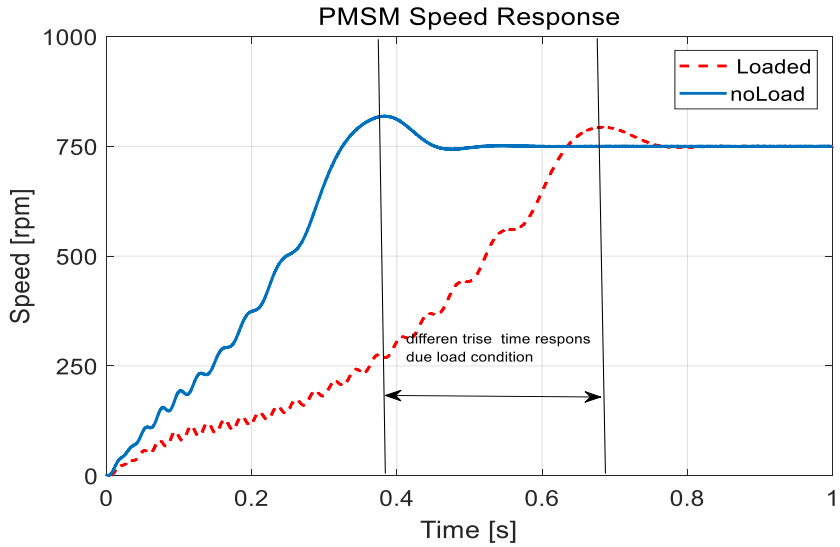

Figure 11: PMSM rotor speeds under variable load conditions in uncontrolled period.

The second approach: The *scaler* control is applied to observe and recover any unstable transient response that appears during variable Load conditions. The speed behaviors have different rise time under load impacts as they demonstrated in the first approach when the machine is not forced to any control algorithm.
In the second approach the PMSM is exposed to the short term transient during the control process. Transient oscillations appear when the speed route passes through the inflection point occurs between positive and negative synchronous speed direction restricted to ±ωr sign. Otherwise, the positive DC voltage in this point declines to zero and the impact of synchronous mode disappear gradually when descended to $\omega_r=0$. After inflection point the speed then begins rising again in negative direction $\omega_r<0$. The speeds are still rolling in the same trajectory even under different loaded conditions due influence of sync-mode. While the control system loses these advantages when the speed reaches to inflection points and causing transient behavior when:

$$\begin{aligned} \omega r > \omega\_sync \quad & + DC\ \ voltage \\ \omega r = \omega\_sync \quad & DC = 0 \\ \omega r < \omega\_sync \quad & - DC\ voltage \end{aligned}$$

These three conditions outlined and determine the characteristics of the transient period, including its duration and the extent of its influence. This angular velocity is shifting the machine from positive (super-synchronous speed) with a positive +D to negative sub-synchronous speed. The depth of this period is influenced by the value of the support DC voltage Figure 12.
Both super-sync and sub-sync can achieve a synchronous characteristic, but when the speed is equal or intersect with synchronous speed, crossing infection point D=0, the transient period starts to perform and the machine speed will respond to load torque conditions again and perform randomly in Figure 13.the duration of transient period started from 10.25ms to 10.8ms with different rise time Tr1=2ms for positive DC boost voltage, and perform longer under loaded machine by Tr2=2.5ms supported with negative DC boost voltage.

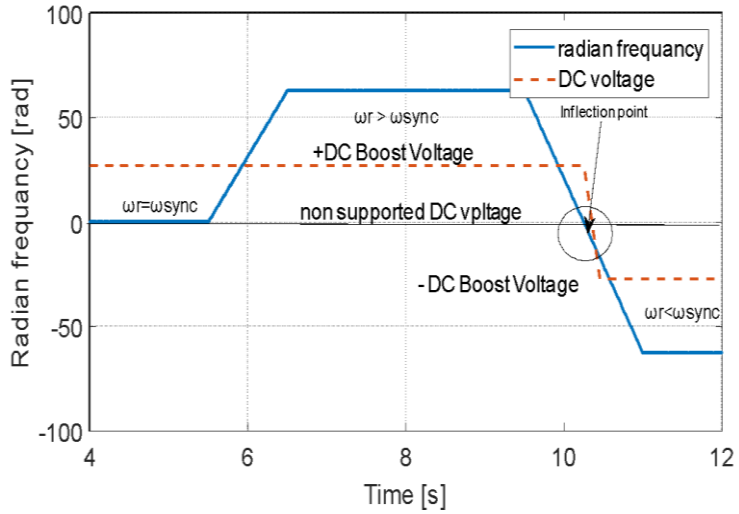

Figure 12: The rotor mechanical rotational speed

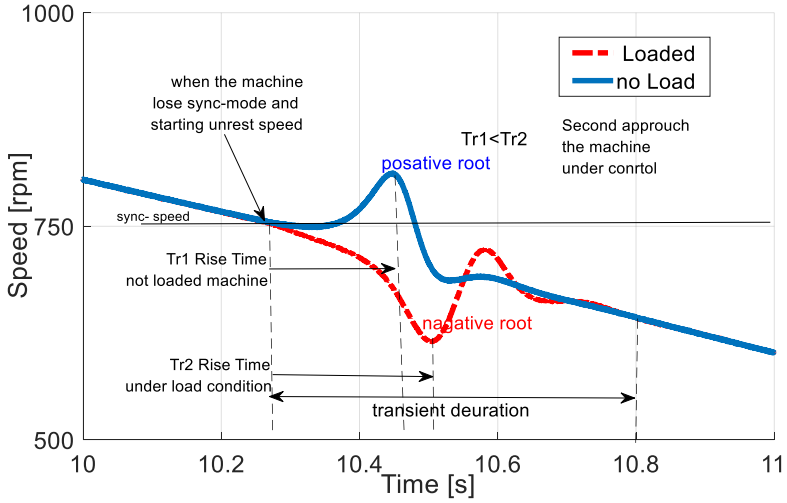

Figure 13: Speed response under controlled mode, the transient appears around the inflection point.

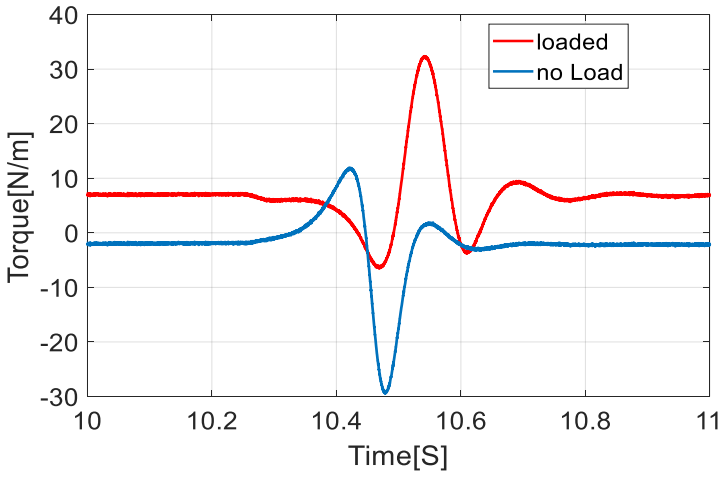

Figure 14: The transient behaviors appear in the variable Torque load condition.

Torque as well responded to variable load conditions. The loaded curve differs from non-loaded torque and record more than 30 N/m, but both cases impacted with short term transient behaviors appear in the zone close inflection point.as it illustrated in figure 14.

The analysis of transients is essential for comprehensively understanding their significant impact on power consumption levels. These transients not only provide critical insights but also serve as compelling evidence of the effectiveness of the control method grounded in the Park hypothesis, particularly in relation to power profiles under varying load conditions. The two perpendicular powers are notably influenced by the transition of speed direction from positive to negative. Furthermore, it is vital to emphasize that Clearfield underscores the pivotal role of supported DC voltage in amplifying the power magnitudes across both load conditions, as illustrated in Figure 15. This insight highlights the intricate relationship between voltage support and power efficiency, making a strong case for careful management of these variables to optimize performance. Showing in figures 15, 16 respectively, these two results are of utmost importance in determining the scope of the transient's influence on power consumption levels. Otherwise, they are considered a proof of the efficiency of the control method supported by the Park hypothesis in reading complex parameters in dq forms accurately. The both perpendicular power are affected by turning point in the speed directions in positive to the negative root. The important note should be Clearfield is the impact of supported DC voltage on magnifying value of active power in the both load conditions.

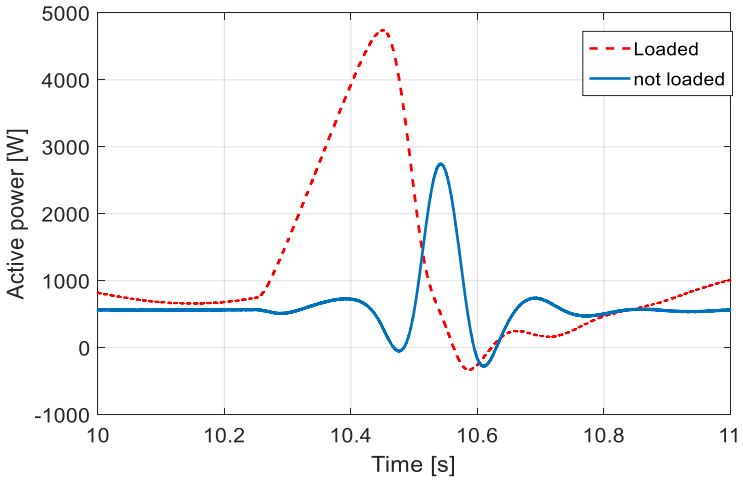

Figure 15: Active power clearly influenced to transient impacts.

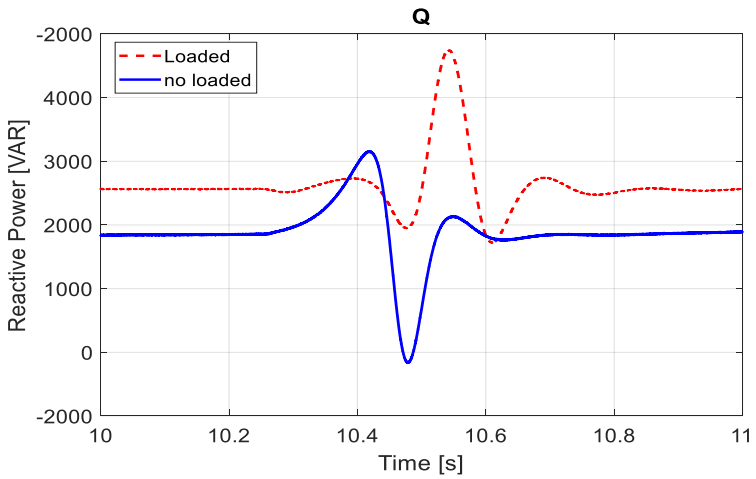

Figure 16: Reactive power responded to deferent loads condition under controlled systems.

The consuming stator currents figure 16 has an essential role to assist the success of control algorithms that reflect obviously electrical variables such as speed; *T, P, and Q* performances are simulated under the same transient time and different load circumstances. The supporting DC voltage also increases the rated current in the positive period and minimizes the negative domain. The short transient period between them tackled serious transient behaviors when the control losing the advantages of synchro mode features, while DC voltage=0 at this cross point, the stator currents' phases twitch inverting to start again in the negative route, as it appear in figure 17. simulation

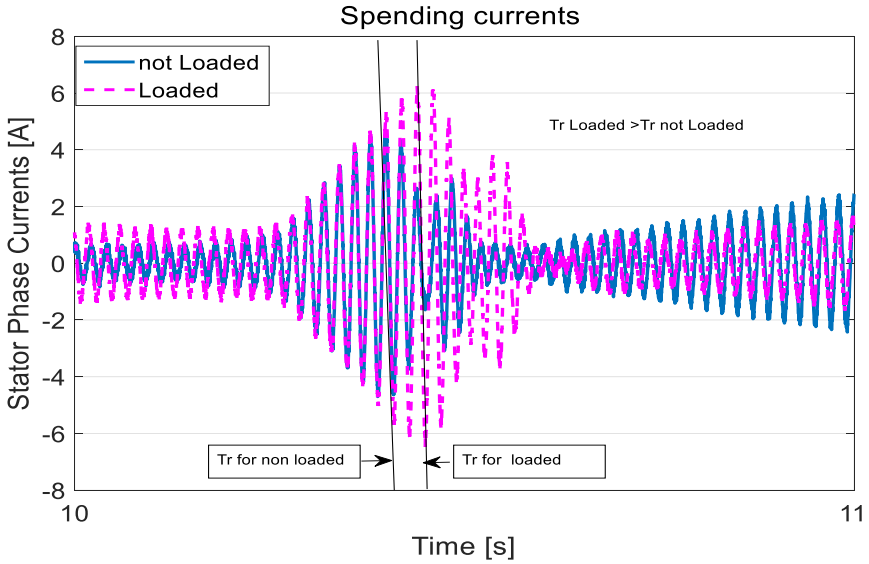

Figure 17: Magnified Transient period-based stator phase currents

6. Conclusions

This paper introduces a high-resolution model of Permanent Magnet Synchronous Motor (PMSM) developed using MATLAB Simulink software. Through comprehensive mathematical analysis, to establish a solid relation between the Park transformation and traditional V/f control, by notable mathematical equation identified transferred the 3ph dynamic model equations to dq form facilitating the construction of a control system to deal with complicated behaviours of transient periods. The parameters such (ωr), electromagnetic torque, (*Tem*), currents (*id* and *iq*), active power and reactive power are enabling thorough exploring of the PMSM characteristics under diverse loading conditions. The adaptability of this model opens up new avenues for examining two transient periods without restrictions, thereby providing invaluable insights into the coupling control method. The higher quality and accuracy of simulation results are evident in the rise time and fall time during transient phases. Our findings reveal a significant advantages will mentioned respectively.

- This research aims to provide a thorough analysis of the transient phase in permanent magnet machines.
- It will examine the duration, underlying causes, and behaviours during variable load changes, in both approaches.
- Additionally, the study seeks to identify effective strategies for enhancing performance during these critical phases, ultimately contributing to improved efficiency and reliability in machine operations.
- Generates a short-term transient state appears such glitches. required to eliminate or minimised. So the approach two established to compere the duration of transient time under deferent load condition.
- The controlled mode minimise the durations of rise time Tr by forcing the

machine to follow ∓DC boost voltage to eliminate unstable change.

- The investigation recorded as well the advantages of scalar control model to minimize transient infects or eliminated torque repels satisfying from DC boost voltage which increase synchronous machine capability to recover un rest periods and follow source frequency during control process .
- This research not only enhances the transient study understanding of PMSMs but also sets a new standard simulation model integrated with parks transformation for future simulations and control strategies in this field.

The Investigation has been proven the success of simulation model's adapted parks transformations hypotheses and absence of synchro-mod based DC boost voltage to minimise the machine's robustness under variable load conditions.

Future work will strategically harness real-time environmental parameters, which are essential for effective process control and enterprise systems. These parameters allow us to operate "without significant delay" in conditions that closely mirror real-time scenarios. The dSPACE platform stands out as the premier real-time environment for testing and validating model code derived from MATLAB simulation software.

References

[1] J. Du, Y. Yuan, and Y. Wei, "Optimization of Permanent Magnet Machine for Electric Vehicles Considering the Control Strategy and Inverter," in *Proc. 23rd Int. Conf. Electr. Machines and Systems (ICEMS)*, 2020, pp. 195–200.

[2] C. J. O'Rourke, M. M. Qasim, M. R. Overlin, and J. L. Kirtley, "A Geometric Interpretation of Reference Frames and Transformations: dq0, Clarke, and Park," *IEEE Trans. Energy Convers.*, vol. 34, no. 4, pp. 2070–2083, Dec. 2019, doi: 10.1109/TEC.2019.2941175.

[3] W. Tong, S. Dai, S. Wu, and R. Tang, "Performance Comparison Between an Amorphous Metal PMSM and a Silicon Steel PMSM," *IEEE Trans. Magn.*, vol. 55, no. 6, pp. 1–5, Jun. 2019.

[4] J. Park, A. G. Vien, M. Cha, T. T. Pham, H. Kim, and C. Lee, "Multiple transformation function estimation for image enhancement," *J. Vis. Commun. Image Represent.*, vol. 95, Art. no. 103863, 2023.

[5] G. Goswami and S. Das, "MTPA Based Energy Efficient Strategy for Scalar Control of Induction Motor Drives," in *Proc. 2024 IEEE 4th Int. Conf. Sustainable Energy Future Electr. Transp. (SEFET)*, Hyderabad, India, Jul. 2024, pp. 1–6, doi: 10.1109/SEFET61574.2024.10717481.

[6] K. K. Dutta, A. Devanshu, and S. Allamsetty, "Scalar-controlled three-phase induction motor drive using FPGA-based WAVECT controller," in *Proc. 2024 3rd Int. Conf. Power Electron. and IoT Applications in Renewable Energy and its Control (PARC)*, Feb. 2024, pp. 264–268.

[7] M. Hassan and M. Jovanovich, "Improved scalar control using flexible DC-Link voltage in Brushless Doubly-Fed Reluctance Machines for wind applications," in *Proc. 2nd Int. Symp. Environ. Friendly Energies and Applications (EFEA)*, Newcastle Upon Tyne, UK, 2012, pp. 482–487, doi: 10.1109/EFEA.2012.6294037.

[8] Y. L. Zhukovskiy, B. Y. Vasilev, and B. Korolev, "The behavior of asynchronous electric drive with a closed scalar control system when changing the inductance of the magnetizing circuit," *Indones. J. Sci. Technol.*, vol. 8, no. 1, pp. 65–78.

[9] B. G. Cho, C. Hong, J. Lee, and W. J. Lee, "Simple position sensorless V/f scalar control method for permanent-magnet synchronous motor drives," *J. Power Electron.*, vol. 21, no. 7, pp. 1020–1029, 2021.

[10] X. Wang et al., "General Modeling and Control of Multiple Three-Phase PMSM Drives," *IEEE Trans. Power Electron.*, 2024.

[11] A. L. O. Vitor, P. R. Scalassara, A. Goedtel, and W. Endo, "Patterns based on Clarke and Park transforms of wavelet coefficients for classification of electrical machine faults," *J.* Control *Autom. Electr. Syst.*, vol. 34, no. 1, pp. 230–245, 2023.

[12] J. Liu and W. Chen, "Generalized DQ model of the permanent magnet synchronous motor based on extended park transformation," *2013 1st International Future Energy Electronics Conference (IFEEC)*, Tainan, Taiwan, 2013, pp. 885-890, doi: 10.1109/IFEEC.2013.6687627.

[13] M. S. Hasan, F. S. Almakhturi, M. D. Albakhait, and A. I. Jaber, "High Performance Rectifier/Multilevel Inverter Based BLDC Motor Drive with PI Controller," *IOP Conf. Ser.: Mater. Sci. Eng.*, vol. 22–23, 2019.

[14] Zhang, P., Shi, Z., Yu, B. and Qi, H., 2024. Research on a sensorless adrc vector control method for a permanent magnet synchronous motor based on the luenberger observer. *Processes*, *12*(5), p.906.

[15] S.-Y. Im, K.-S. Cha, Y.-J. Won, Y.-Y. Choi, and M.-S. Lim, "Two-Step Optimum Design Process of PMSM to Improve Driving Efficiency and

Harmonics of Lightweight Electric Vehicle," *IEEE Trans. Ind. Appl.*, 2023.

[16] C.-S. Park, J.-H. Kim, S.-H. Park, and M.-S. Lim, "Effect of electromagnetic force caused by PMSM on the vibration/noise of reciprocating compressors," *IEEE Access*, vol. 11, pp. 56324–56335, 2023;

[17] Krupa, T. M., et al. "Interior Permanent Magnet Synchronous Motor for EV Applications." *2024 8th International Conference on Computational System and Information Technology for Sustainable Solutions (CSITSS)*. IEEE, 2024.

[18] H. S. Hameed, Q. Al Azze, and M. S. Hasan, "Speed control of switched reluctance motors based on fuzzy logic controller and MATLAB/Simulink," *Indones. J. Electr. Eng. Comput. Sci.*, vol. 31, no. 2, pp. 647–657, 2023.

[19] Song, Won Seok, and Seungjae Min. "Robust topology optimization of interior permanent magnet synchronous motor for torque ripple reduction under current uncertainty." *Applied Mathematical Modelling* 140 (2025): 115917..

[20] Z. He and T. Shinshi, "Torque Regulation Theory and Sensorless Control Technology for Unipolar Salient Synchronous Permanent Magnet Motor Based on Unified Models," in *IEEE Transactions on Power Electronics*, vol. 40, no. 4, pp. 5672-5684, April 2025, doi: 10.1109/TPEL.2024.3495715

[21] G. Yun, Y. Choo, C. Kim, S. Lee, D.-K. Hong, and C. Lee, "Vibration analysis of a permanent magnet synchronous motor by a pole/slot combination," *AIP Adv.*, vol. 13, no. 2, 2023.

[22] R. A. Mejeed, M. S. Hasan, A. I. Jaber, and A. N. Almakki, "New Scheming Approach of Switching Gates Based DC-Link Controller," in *Proc. 2023 Seminar Ind. Electron. Devices Syst. (IEDS)*, Saint Petersburg, Russia, 2023, pp. 177–180, doi: 10.1109/IEDS60447.2023.10425998.

[23] R. Bharti, M. Kumar, and B. M. Prasad, "V/F Control of Three Phase Induction Motor," in *Proc. 2019 Int. Conf. Vision Towards Emerging Trends Commun. Netw. (ViTECoN)*, Vellore, India, 2019, pp. 1–4, doi: 10.1109/ViTECoN.2019.8899420.

[24] J. Liu and W. Chen, "Generalized DQ model of the permanent magnet synchronous motor based on extended Park transformation," in *Proc. 2013 1st Int. Future Energy Electron. Conf. (IFEEC)*, Tainan, Taiwan, 2013, pp. 885–890, doi: 10.1109/IFEEC.2013.6687627.

[25] M. Inoue and S. Doki, "PMSM Model Discretization in Consideration of Park Transformation for Current Control System," in *Proc. 2018 Int. Power Electron. Conf. (IPEC-Niigata 2018 -ECCE Asia)*, Niigata, Japan, 2018, pp. 1228–1233, doi: 10.23919/IPEC.2018.8507948.

[26] Y.-R. Lee and S.-K. Sul, "Switching Frequency Signal-Injection Sensorless Control in Dual Three-Phase PMSM Robust to Non-Ideal Characteristics of Inverter System," *IEEE Trans. Power Electron.*, 2024.

[27] C. Chen, Y. Chen, X. Yang, S. Gao, and B. Zhang, "Inverter Fault Detection Method Based on Park Transformation and K-means Clustering Algorithm," in *Proc. 2021 CAA Symp. Fault Detection, Supervision, and Safety Tech. Process. (SAFEPROCESS)*, Chengdu, China, 2021, pp. 1–6, doi: 10.1109/SAFEPROCESS52771.2021.9693715.

[28] F. V. Lopes, D. Fernandes, and W. L. A. Neves, "A Traveling-Wave Detection Method Based on Park's Transformation for Fault Locators," *IEEE Trans. Power Del.*, vol. 28, no. 3, pp. 1626–1634, Jul. 2013, doi: 10.1109/TPWRD.2013.2260182.

[29] S. A. Kim, J. H. Song, S. W. Han, and Y. H. Cho, "An Improved Dynamic Modeling of Permanent Magnet Synchronous Machine with Torque Ripple Characteristics," *J. Clean Energy Technol.*, vol. 6, no. 2, p. 4, 2018.

[30] M. A. Rahman and T. A. Little, "Dynamic Performance Analysis of Permanet Magnet Synchronous Motors Magnet Synchronous Motors," in IEEE Transactions on Power Apparatus and Systems, vol. PAS-103, no. 6, pp. 1277-1282, June 1984, doi: 10.1109/TPAS.1984.318460.